Fibrocontractive Müller Cell Phenotypes in Proliferative Diabetic Retinopathy

Clyde Guidry, Jeffery L. King, and John O. Mason III

Purpose. To evaluate Müller cells as a potential source of fibrocontractive cells in proliferative diabetic retinopathy.

Methods. Temporal changes in glial fibrillary acidic protein (GFAP), vimentin, glutamine synthetase, and alpha smooth muscle actin (αSMA) expression in cultures of freshly isolated porcine Müller cells were evaluated by indirect immunofluorescence and Western blotting. A similar evaluation was performed on freshly isolated Müller cells maintained in high- and low-glucose culture. Cryosections of six diabetic epiretinal tissues were evaluated for the same antigens.

Results. Müller cell changes in culture included loss of glutamine synthetase and GFAP, with coincident gains in αSMA immunoreactivity. Vimentin immunoreactivity persisted without obvious change. Similar changes were observed when the cells were maintained in high- or low-glucose culture medium. All six diabetic epiretinal membranes contained positively identified Müller cells with vimentin, GFAP, and glutamine synthetase immunoreactivities. There was a progressive loss of glutamine synthetase and GFAP content and a coincident increase in αSMA content as the cells assumed an elongated, fibroblastlike morphology.

Conclusions. Continuous culture in high- versus low-glucose medium does not influence Müller cell phenotype changes. Positively identified Müller cells are present in diabetic epiretinal tissues and appear to undergo the same progression of phenotype changes observed in culture. Cells capable of generating tractional forces associated with proliferative diabetic retinopathy can arise from Müller cells. (*Invest Ophthalmol Vis Sci.* 2009;50:1929–1939) DOI:10.1167/iovs.08-2475

Proliferative diabetic retinopathy (PDR) is a common late or end-stage complication of diabetes, the frequency of which increases with disease duration and severity.[1] Fibrovascular tissue emerges from the retina into the vitreal space, and tractional forces originating within this tissue threatens the retinal anatomy, necessitating surgical intervention. PDR is a cellular disorder in that its pathogenesis involves an identifiable progression of activities including cell translocation from the retina, increase in cell number through mitosis, and tractional force generation through extracellular matrix contraction.[2]

Immunocytochemical studies performed in the past two decades have identified a number of different cells in diabetic epiretinal tissues, including retinal glia,[3–5] macrophages,[6] microglia,[7] and retinal pigment epithelial cells.[8] Interestingly, despite the information available, the identities of the principal effector cells—those actually causing traction retinal detachments—are still unknown. Effective tractional force generation requires expression of the myoid marker alpha smooth muscle actin (αSMA).[9] Consistent with this mechanistic requirement, a number of investigators reported detecting αSMA-positive cells in diabetic epiretinal tissue.[10–12] However, because of the superficial similarity to connective tissue fibroblasts, these cells were described as fibrocytes, fibroblasts, or myofibroblasts.[3,10–14] To date, no experimental evidence has been offered to support a connective tissue origin for these cells, making their identification as myofibroblasts speculative.

Studies from this laboratory reported that primary Müller cells, maintained in tissue culture, develop the capacity to generate tractional forces.[15] This activity arises during a progression of immunochemical changes that include loss of GFAP content and de novo expression of αSMA, resulting in a fibroblastlike cell that is unrecognizable as of glial origin.[16] The pathogenic relevance and contributions of Müller cell-derived fibroblasts to diabetic traction retinal detachment are uncertain because the presence of these cells in diabetic epiretinal tissues has not yet been evaluated experimentally. This study tested the hypothesis that Müller cell-derived fibroblasts contribute to the population of cells capable of generating tractional forces in PDR. Systematic comparisons of Müller cells in culture and diabetic epiretinal membranes were performed to examine early phenotype changes in culture and to better define temporal intermediates using a broader panel of antigens. These data were used to evaluate the presence of immunochemically identifiable Müller cells in diabetic epiretinal membranes and to determine if a similar progression of phenotype changes occurs in disease.

Methods

Isolation and Culture of Porcine Müller Cells

Müller cells were isolated from normal porcine retina and maintained in culture using previously published methods.[15] The methods used to secure animal tissues complied with the ARVO Statement for the Use of Animals in Ophthalmic and Vision Research and were approved by the Institutional Review Board at the University of Alabama at Birmingham. Briefly, eyes removed from anesthetized animals were maintained in ice-cold saline until dissection. Retinas were digested sequentially with papain and DNase, and the cells were released by repeated trituration. Supernatants enriched with morphologically recognizable Müller cells were combined and plated in growth medium composed of Dulbecco's minimum essential medium (DMEM) supplemented with 20 mM N-2-hydroxyethylpiperazine-N-2-ethanesulfonic acid and 10% fetal bovine serum. The cells were permitted to adhere for 30 to 60 minutes at 37°C, after which the nonadherent population was removed and the medium was replaced with fresh growth medium. Müller cell phenotypes in culture were evaluated by indirect immunofluorescence of fixed, permeabilized cells attached to glass coverslips using polyclonal rabbit anti–GFAP and mouse monoclonal anti–αSMA an-

From the Department of Ophthalmology, University of Alabama School of Medicine, Birmingham, Alabama.

Supported by the International Retinal Research Foundation and by National Eye Institute Grant EY013258.

Submitted for publication June 23, 2008; revised September 24, November 24, and December 1, 2008; accepted February 27, 2009.

Disclosure: **C. Guidry**, None; **J.L. King**, None; **J.O. Mason III**, None

The publication costs of this article were defrayed in part by page charge payment. This article must therefore be marked "*advertisement*" in accordance with 18 U.S.C. §1734 solely to indicate this fact.

Corresponding author: Clyde Guidry, Department of Ophthalmology, University of Alabama School of Medicine, CEFH DB106, Birmingham, AL 352994; cguidry@uab.edu.

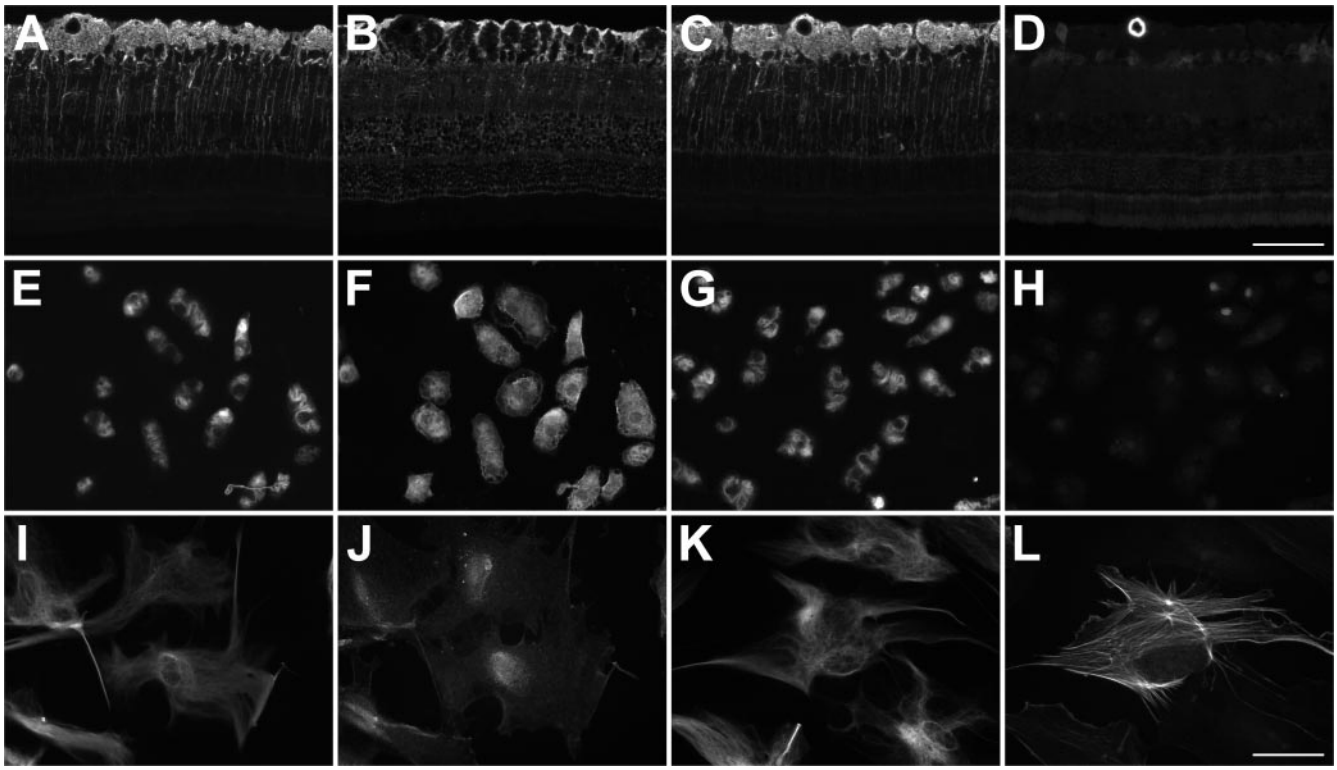

FIGURE 1. Indirect immunofluorescence evaluation of Müller cell changes in culture. Cryosections of normal porcine retina (**A–D**) and freshly isolated Müller cells maintained in culture for 1 (**E–H**) and 7 (**I–L**) days were double probed with antibodies against GFAP (**A**, **E**, **I**) and glutamine synthetase (**B**, **F**, **J**) or GFAP (**C**, **G**, **K**) with αSMA (**D**, **H**, **L**) and were detected using fluorochrome-conjugated secondary antibodies. Scale bars: 100 μm (**A–D**); 50 μm (**E–L**).

tibodies, as described previously.[16] Cultures were maintained in a humidified incubator at 37°C with growth medium changes every 3 to 4 days until confluence, when they were released with 0.05% trypsin and 0.53 mM EDTA and replated in fresh growth medium.

An additional Müller cell isolation was performed using two retinas harvested from the same animal. Cells were isolated as described but were maintained in DMEM formulations that were identical except for high (5 g/L; #1288–017; Invitrogen, Carlsbad, CA) and low (1 g/L; #31600–034; Invitrogen) glucose. Both formulations were supplemented with 20 mM N-2-hydroxyethylpiperazine-N-2-ethanesulfonic acid and 10% fetal bovine serum. Cell phenotypes were evaluated by indirect immunofluorescence as described after 2 hours, 7 days, and 14 days in culture.

Cell and Tissue Processing for Immunofluorescence Microscopy

Cells attached to coverslips were fixed with 2% paraformaldehyde in phosphate buffer (0.1 M Na_2 HPO_4, pH 7.0) for 1 hour at room temperature, washed with phosphate-buffered saline (PBS; 0.01 M Na_2HPO_4, 0.15 M NaCl, pH 7.4), and permeabilized by 10-minute treatment with PBS containing 0.1% Triton X-100. Normal porcine ocular tissue was harvested and prepared using previously published methods.[16] Intraocular scar tissue was removed during the normal course of surgery to correct PDR. Informed consent was obtained from all persons involved in this project, in accordance with the tenets of the Declaration of Helsinki. Tissue was fixed for 1 hour at 4°C with 2% paraformaldehyde in phosphate buffer, rinsed with additional phosphate buffer, infiltrated for 1 hour on ice with 1 part frozen tissue-embedding media (FisherDiagnostics, Fair Lawn, NJ) and 2 parts 30% sucrose in phosphate buffer, and quick frozen with cryospray. All specimens were sectioned in their entirety, with four 5-μm cryosections placed on each slide. Every tenth slide (4–6

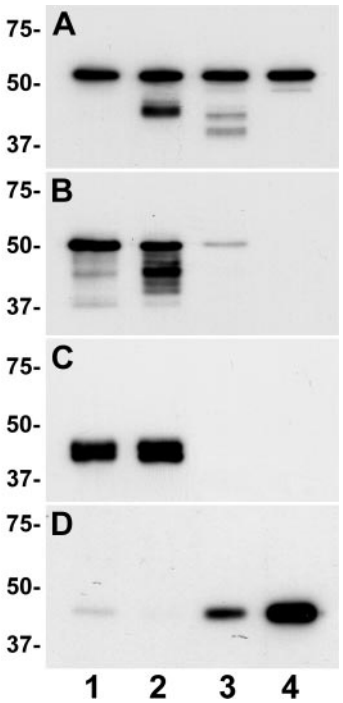

FIGURE 2. Evaluation of Müller cell changes by Western blotting. Detergent-extracted proteins from normal porcine retina (*lane 1*) and freshly isolated Müller cells maintained in culture for 1 day (*lane 2*), 7 days (*lane 3*), and 35 days (*lane 4*) were probed in Western blots using antibodies against vimentin (**A**), GFAP (**B**), glutamine synthetase (**C**), and αSMA (**D**).

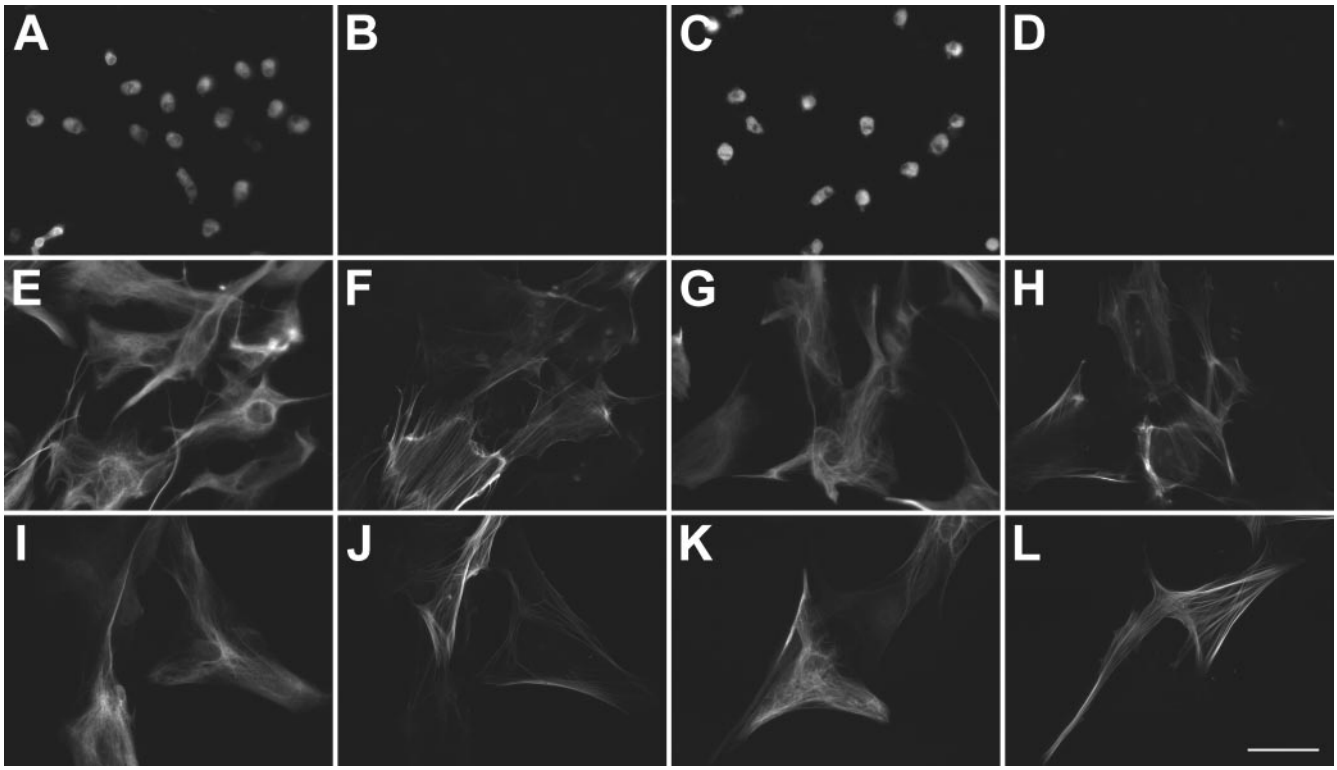

FIGURE 3. Indirect immunofluorescence evaluation of Müller cell changes in high- and low-glucose culture medium. Freshly isolated Müller cells in high- (**A**, **B**, **E**, **F**, **I**, **J**) and low- (**C**, **D**, **G**, **H**, **K**, **L**) glucose medium were incubated for 2 hours (**A–D**), 7 days (**E–H**), and 14 days (**I–L**). Coverslips were double probed with antibodies against GFAP (**A**, **C**, **E**, **G**, **I**, **K**) and αSMA (**B**, **D**, **F**, **H**, **J**, **L**) and were detected using fluorochrome-conjugated secondary antibodies. Scale bar, 50 μm.

slides per specimen) was stained with hematoxylin to evaluate cell distribution and to identify the regions of interest presented in the Results (see Fig. 3). Cryosections and coverslips were blocked with 20% nonimmune goat serum (The Binding Site, Ltd., Birmingham, UK) in PBS for 60 minutes at room temperature. Primary and secondary antibody treatments were for 60 minutes at room temperature using 2% goat serum in PBS with three 5-minute washes in between. Four slides immediately above the region of interest were stained with individual antibodies against GFAP, vimentin, glutamine synthetase, and αSMA. Double-staining experiments were performed on the three slides immediately below the region of interest. Photomicrographs were taken with a microscope equipped with epifluorescence illumination and phase-contrast optics (Optiphot; Nikon, Tokyo, Japan) and with a digital camera (RETIGA EXi; QImaging Corp., Burnaby, BC, Canada). Images were assembled into composite photographs with image management software (Photodeluxe; Adobe Systems, Inc., San Jose, CA).

Changes in tissue-associated pixel intensities associated with the different immunoprobes were evaluated using unaltered images taken with the same 40× objective under exposure conditions specific for each immunoprobe. Tissue sections were masked, and mean tissue-associated pixel intensities above background were calculated using the histogram statistics function in commercial software (Adobe Photoshop C2; Adobe Systems, Inc.). At least three exposures for each antigen were evaluated for each sample.

Western Blot Analysis

Western blot analysis was performed on detergent-extracted proteins from Müller cell cultures and porcine retina, separated on 5% to 15% SDS-PAGE gels under reducing conditions, and transferred to polyvinylidene difluoride membranes (Hybond-P; GE Healthcare) for 60 minutes at 100 V.[17] The membranes were blocked with 5% nonfat dry milk (Bio-Rad, Hercules, CA) in PBS with 0.1% Tween-20 (PBST, pH 7.5) and probed with primary and secondary antibodies diluted in PBST for 60 minutes each with three 10-minute washes in between. Insulin-like growth factor binding protein (IGFBP) Western blot membranes were blocked with 3% nonfat dry milk in TBST for 60 minutes at room

TABLE 1. Differential Müller Cell Changes in Response to High- and Low-Glucose Medium

	High Glucose		Low Glucose		*P*	
	7 Days	14 Days	7 Days	14 Days	7 Days	14 Days
GFAP	94.0 ± 3.5	42.8 ± 10.3	93.6 ± 1.4	52.6 ± 5.0	0.25	0.19
Vimentin	95.2 ± 3.4	96.4 ± 5.2	96.4 ± 5.2	99.1 ± 1.6	0.24	0.13
Glutamine synthetase	3.7 ± 3.4	0.0 ± 0.0	2.0 ± 1.9	0.0 ± 0.0	0.25	0.21
αSMA	90.2 ± 4.5	89.1 ± 7.8	86.9 ± 2.5	93.6 ± 5.8	0.19	0.37

Values are presented as % positive cells ± SD. *P* values for high- versus low-glucose medium at both time points were calculated using the Student's *t*-test.

temperature, and IGFBP was detected with primary and horseradish peroxidase-conjugated secondary antibodies diluted in blocking solution for 60 minutes each. Chemiluminescence detection was conducted (Super Signal West Femto; Pierce, Rockford, IL) according to the manufacturer's instructions, and the membranes were exposed to autoradiographic film (Super Rx; Fuji Film Company Ltd., Tokyo, Japan).

Reagents

Tissue culture media and serum were obtained from Life Technologies (Rockville, MD). Antibodies were obtained from commercial suppliers and included rabbit anti–GFAP (Dako, Glostrup, Denmark), mouse anti–αSMA (clone 1A4; Sigma Chemical Co., St. Louis, MO), mouse anti–vimentin (clone V9; Dako), mouse anti–glutamine synthetase (MAB302; Chemicon International, Inc., Temecula, CA), rhodamine-conjugated goat anti–mouse IgG (Jackson ImmunoResearch Laboratories, West Grove, PA), Cy2-conjugated goat anti–rabbit IgG (Jackson), horseradish peroxidase-conjugated goat anti–mouse IgG (Jackson), and horseradish peroxidase-conjugated goat-anti–rabbit IgG (Jackson) antibodies. Normal goat serum was obtained from Jackson ImmunoResearch Laboratories, and other chemicals and reagents were obtained from Sigma.

Results

Müller Cell Phenotype Changes in Culture

To examine glutamine synthetase expression in relation to GFAP, vimentin, and αSMA, freshly isolated porcine Müller cells were maintained in culture for varying lengths of time and then probed with the use of indirect immunofluorescence. As we reported previously, Müller cells in retina and all tissue culture stages were strongly positive for vimentin (not shown).[15,16] Normal retina probed with antibodies against GFAP revealed astrocytes and radially oriented Müller cells (Fig. 1A), whereas glutamine synthetase labeling was limited to Müller cells alone (Fig. 1B, same field as 1A). In contrast, the adjacent section probed for GFAP and αSMA was similarly positive for GFAP (Fig. 1C) but negative for αSMA except for vascular myocytes (Fig. 1D, same field as 1C). Freshly isolated Müller cells maintained in culture for 1 day had similar patterns of immunoreactivity in that all cells were positive for GFAP and glutamine synthetase (Figs. 1E and 1F, same fields) and negative for αSMA (1H, same field as 1G). Cells maintained in culture for 7 days were of an intermediate phenotype in that the cells were less strongly positive for GFAP and had little or no glutamine synthetase-associated signal (Figs. 1I and 1J, same field). In contrast, the cells were now variably positive for αSMA and, in some cases, had prominent stress fibers (Figs. 1K and 1L, same field). Finally, as previously reported, Müller cells at 35 days in culture (passage 5) were uniformly negative for GFAP and positive for αSMA (not shown).[15,16] These cells were also negative when probed for the presence of glutamine synthetase (not shown).

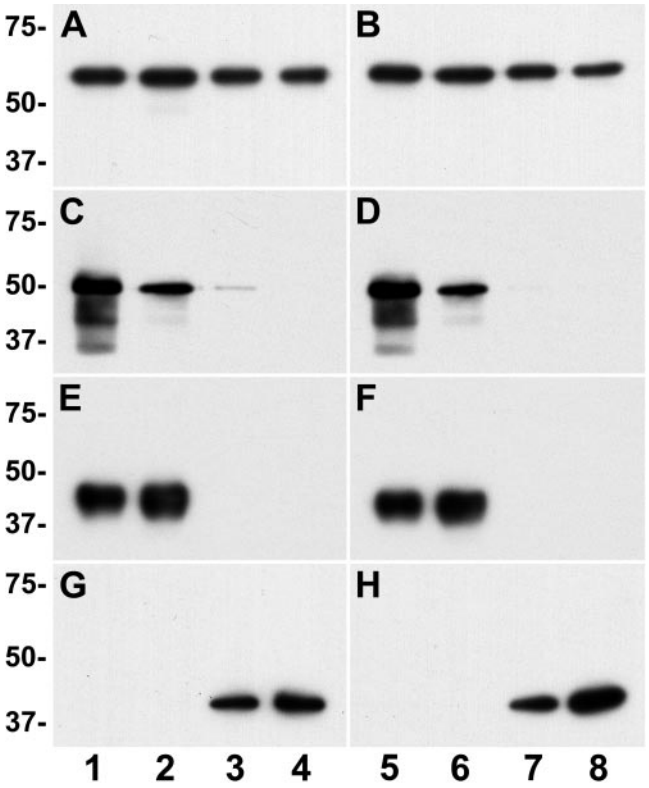

Figure 4. Evaluation of Müller cell changes in response to high- and low-glucose medium by Western blotting. Detergent-extracted proteins from normal porcine retina (*lanes 1, 5*) and freshly isolated Müller cells maintained in high- (*lanes 2–4*) and low- (*lanes 6–8*) glucose medium after 2 hours (*lanes 2, 6*), 7 days, (*lanes 3, 7*), and 14 days (*lanes 4, 8*) were probed in Western blots using antibodies against vimentin (**A**, **B**), GFAP (**C**, **D**), glutamine synthetase (**E**, **F**), and αSMA (**G**, **H**).

Table 2. Clinical Demographics of Patients

Diagnosis	Diabetic traction retinal detachment
Mean diabetes duration	19 years (range, 6–32)
Diabetes	
Type 1 IDDM	4
Type 2 NIDDM	2
Mean age	62 years (range, 42–76)
Sex	
Male	4
Female	2

IDDM, insulin-dependent diabetes mellitus; NIDDM, non-insulin-dependent diabetes mellitus.

In parallel studies to confirm the immunocytochemical observations, protein extracts from normal porcine retina and Müller cells at the different culture stages were evaluated in Western blots using the same immunoprobes. Müller cells in retina and all cell cultures were strongly positive for vimentin, and cell extracts were normalized to produce vimentin staining of comparable intensity (Fig. 2A). A similar evaluation using antibodies against β-actin produced comparable results (not shown). Retinal and Müller cell extracts from 1-day cultures were strongly positive for GFAP, with significant signal loss apparent by 7 days (Fig. 2B). Similarly, retina and 1-day lysates were strongly positive for glutamine synthetase, but this protein could not be detected after 7 days in culture (Fig. 2C). In contrast, only trace quantities of αSMA could be detected in normal retina, but the cultures were positive by 7 days with additional increases in longer term cultures (Fig. 2D). These results revealed a temporal progression of antigen changes in Müller cells in that glutamine synthetase loss precedes that of GFAP. In turn, αSMA expression was not pronounced until after glutamine synthetase loss, and vimentin expression appeared to remain unchanged in all phenotypes.

High-Glucose Culture Medium on Müller Cell Phenotype Changes

In response to reviewer concerns about the effects of high-glucose culture medium on Müller cell phenotype changes,

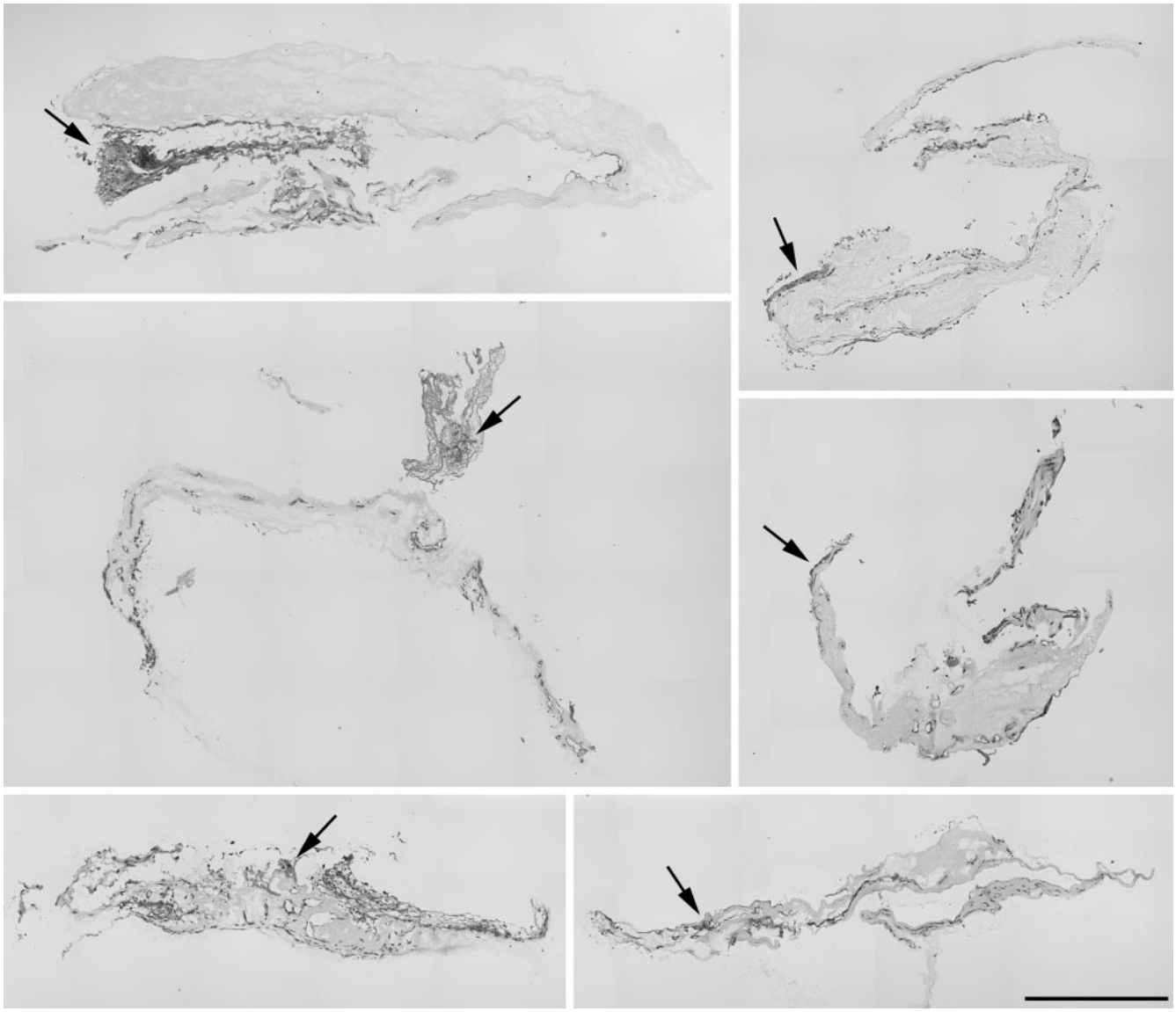

FIGURE 5. Photomontages of human epiretinal membranes. Cryosections of human epiretinal scar were probed with hematoxylin and were photographed and assembled into low-magnification photomontages. *Arrows*: regions of intensely stained cells in high density. Scale bar, 500 μm.

we performed another Müller cell isolation and characterization using two retinas harvested from the same animal. After dissection and papain digestion in glucose-free L15 medium, the freshly dissociated Müller cells were suspended and maintained in DMEM containing high (5 g/L) or low (1 g/L) glucose. After 2 hours of incubation, cells under both conditions were fixed, permeabilized, and probed with the same antibody combinations used in Figure 1. The cells were uniformly positive for GFAP (Figs. 3A, 3C), negative for αSMA (Figs. 3B, 3D; same fields as 3A and 3C), and positive for glutamine synthetase (not shown) and vimentin (not shown). A similar evaluation performed after 7 days in culture revealed that the now well-spread cells were heterogeneous in GFAP expression in high-glucose (Fig. 3E) and low-glucose (Fig. 3G) media. Expression of αSMA and assembly into stress fibers was also evident in high-glucose (Fig. 3F, same field as 3E) and low-glucose (Fig. 3H, same field as 3G) media. Cells under both conditions were uniformly negative for glutamine synthetase (not shown) and positive for vimentin (not shown). Yet another evaluation performed after 14 days in culture revealed that the cells maintained in high-glucose (Fig. 3I) and low-glucose (Fig. 3K) media were still heterogeneous for GFAP content though the staining was considerably less intense. Cells and associated stress fibers were also heterogeneously positive for αSMA (Figs. 3J and L, same fields as 3I and 3K), though in this case the staining was more intense. In addition, as earlier, the cells were homogeneously negative for glutamine synthetase and positive for vimentin. Müller cell changes were quantified by an observer (JLK) masked to the experimental conditions, grading the cells as either positive or negative during a north to south transit of each coverslip counting a minimum of 100 cells in three complete fields. The results, presented in Table 1, are consistent with the progressive loss of GFAP, gain in αSMA, and loss of glutamine synthetase expression presented in Figure 3.

Finally, in parallel studies to confirm the immunocytochemical observations, protein extracts from normal retina

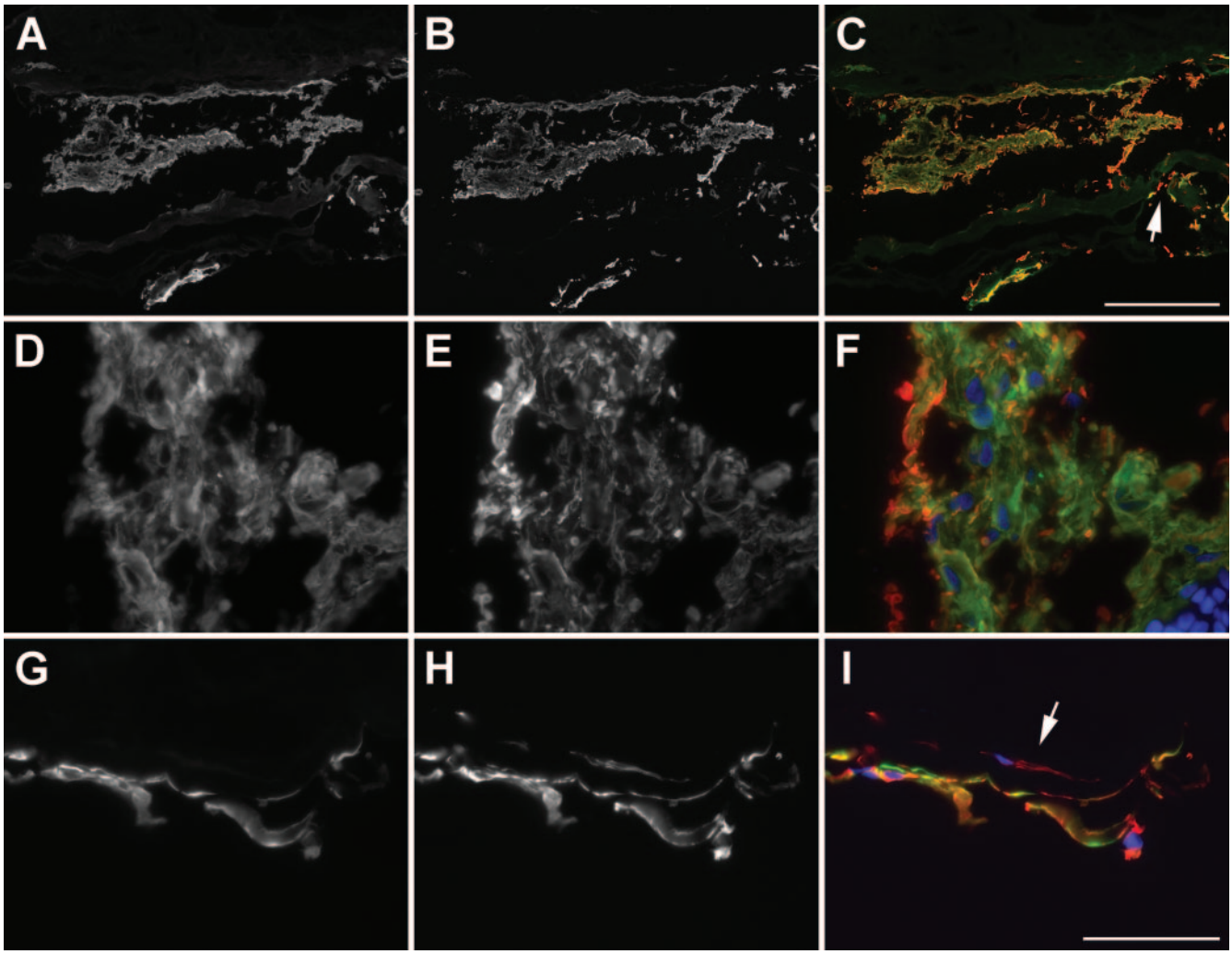

Figure 6. Indirect immunofluorescence evaluation of GFAP and vimentin distribution in epiretinal scar. Cryosections adjacent to that presented in Figure 3 were probed with antibodies against GFAP (**A**, **D**, **G**) and vimentin (**B**, **E**, **H**) and detected with fluorochrome-conjugated secondary antibodies. Nuclei were labeled with DAPI. Merged images (**C**, **F**, **I**) contain three color channels representing DAPI (*blue*), GFAP (*green*), and vimentin (*red*). Scale bars: 250 μm (**A–C**); 50 μm (**D–I**).

and these same cultures were evaluated in Western blots using equal lysate volumes from the paired high- and low-glucose cultures and the same immunoprobes. Müller cells in retina, from high-glucose and low-glucose cultures, were strongly positive for vimentin. Retinal and Müller cell extracts from both cultures were also strongly positive for GFAP, with significant signal loss apparent by 7 and 14 days (Figs. 4C, 4D). Similarly, retina and 2-hour lysates were strongly positive for glutamine synthetase, but this protein could not be detected after 7 days in culture under either condition (Figs. 4E, 4F). In contrast, under these conditions, αSMA was not detected in normal retina or 2-hour cultures, but the cultures were positive by 7 days (Figs. 4G, 4H). Taken together, these data indicate that continuous culture in media containing high or low glucose does not influence stress fiber formation or the previously described changes in Müller cell phenotype.

Müller Cells in Fibrocontractive Epiretinal Membranes

Epiretinal scars removed during corrective surgery (Table 2) were first evaluated for cell density and distribution. Samples were fixed, cryopreserved, and sectioned, and every tenth slide (4–6 slides per sample) was stained with hematoxylin and evaluated by light microscopy. Photomicrographs were taken of the slides with the highest apparent cell densities and, to permit direct comparisons, were assembled into photocomposites (Fig. 5). Although the overall organization and distribution of cells varied, every specimen contained one or more regions of darker staining, tightly packed cells (Fig. 5, arrows) and areas of lower cell densities.

We evaluated the presence and distribution of glia using slides adjacent to those presented in figure 5, double probed with antibodies against GFAP and vimentin. Presented in Figure 6 are composite photomicrographs of the large, darkly stained mass demonstrated in Figure 5 (top left panel). At this magnification, all cells in the high-density mass appeared to be intensely positive for GFAP (Fig. 6A) and vimentin (Fig. 6B). Although many cells peripheral to the high-density mass were also positive for both antigens, GFAP reactivity appeared to be less intense. These differences were most easily detected in merged images in which the reduced GFAP fluorescence yielded orange to red cells

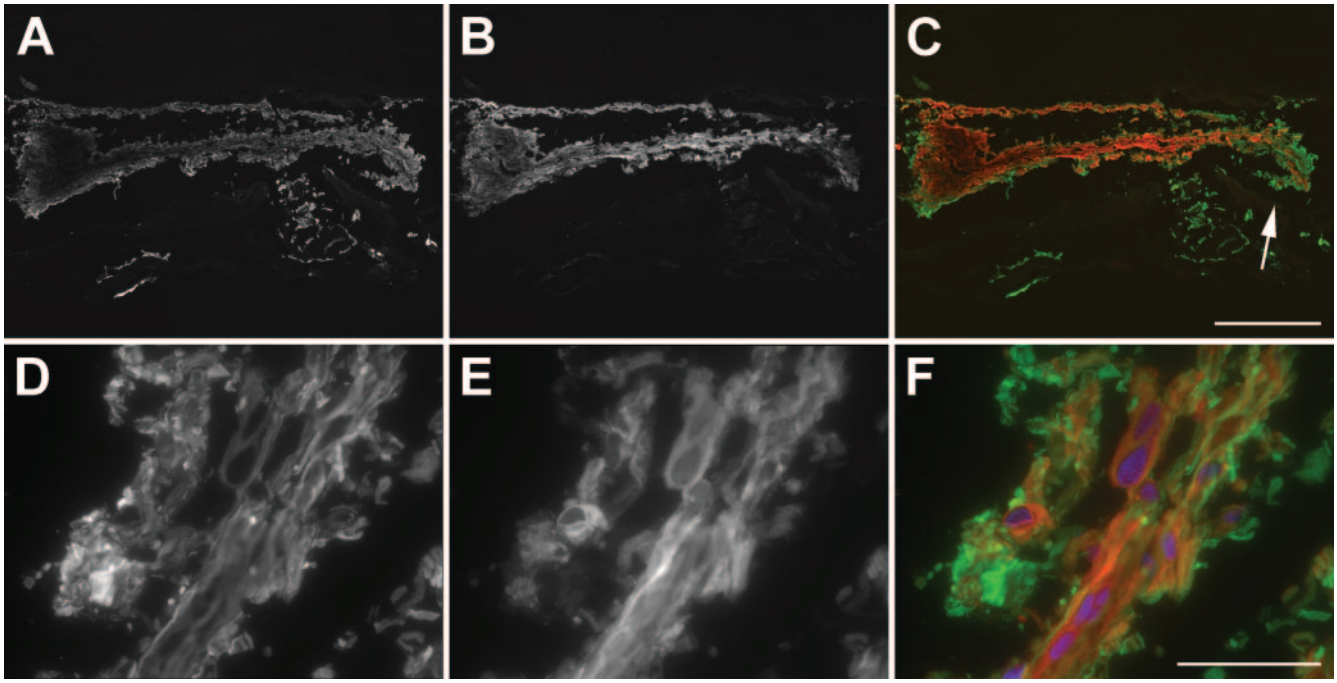

FIGURE 7. Indirect immunofluorescence evaluation of GFAP and glutamine synthetase distribution in human epiretinal scar. Cryosections adjacent to those presented in Figure 3A were probed with antibodies against GFAP (**A**, **D**) and glutamine synthetase (**B**, **E**) and were detected using fluorochrome-conjugated secondary antibodies. Nuclei were detected using DAPI. Merged images (**C**, **F**) contain three color channels representing DAPI (*blue*), GFAP (*green*), and glutamine synthetase (*red*). Scale bars: 250 μm (**A–C**); 50 μm (**D–F**).

(Fig. 6C, arrow). Higher magnification views of the same sample confirmed these observations at the level of individual cells. Although the distribution and intensity of GFAP and vimentin fluorescence varied in the high-density mass, evaluation of individual (Figs. 6D, 6E) and merged (Fig. 6F) images revealed that all cells in these areas were positive for both antigens. However, this was not the case for the elongate, fibroblastlike cells in the periphery. Although many cells were variably positive for GFAP (Fig. 6G), vimentin-positive cells (Fig. 6H) with little or no GFAP reactivity were also detectable in the same field (Fig. 6I, arrow), a finding consistent with cells in transition.

To distinguish between Müller and astrocytic glia, slides were also double probed with antibodies against GFAP and glutamine synthetase. As before, in low-magnification photocomposites, GFAP reactivity was present in high- and low-cell density zones (Fig. 7A). In contrast, glutamine synthetase reactivity was more restricted, limited to regions of high cell density (Fig. 7B). Evaluation of the merged images was also suggestive of cells in transition, with progressive loss of glutamine synthetase reactivity in cells peripheral to the high-density mass (Fig. 7C, arrow). High-magnification views of the transition zone supported this premise in that all cells in the image were positive for GFAP (Fig. 7D) whereas glutamine synthetase reactivity was most evident in the centrally located cells (Fig. 7E). As earlier, regional differences in cell-specific antigen intensity were more apparent in merged images (Fig. 7F).

To determine which, if any, of the cells were capable of generating tractional forces, slides from these same regions were also double probed with antibodies against αSMA and GFAP. As earlier, GFAP reactivity was present in the high-density cell mass and in occasional cells in the periphery (Fig. 8A). In contrast, intense SMA reactivity was limited to peripheral cells and was only weakly detected in the high-density mass (Fig. 8B). Merged images at this magnification revealed no obvious overlap in the intensely labeled cells (Fig. 8).

High-magnification views of these specimens revealed a more complex relationship. Müller cells in the high-density mass were intensely positive for GFAP (Fig. 9A), but were also positive for αSMA in the form of punctate staining and occasional circular structures (Fig. 9B, arrow). Merged images with DAPI-labeled nuclei revealed the circular structures to be perinuclear rings (Fig. 9C). Cells in the glutamine synthetase transition zone (demonstrated in Fig. 7F) were still positive for GFAP (Fig. 9D) and had generally increased αSMA content (Fig. 9E) in that virtually all cells had αSMA-positive perinuclear rings that were also apparent in merged images (Fig. 9F). Scrutiny of the low-density zones revealed regions of elongate, fibroblastlike cells positive for both antigens. In this case GFAP labeling was comparatively weak (Fig. 9G), and αSMA reactivity occurred in the form of short, intensely positive stress fiberlike structures aligned on only one side of the nucleus (Fig. 9H). Merged images with DAPI-labeled nuclei confirmed the localization of both antigens to individual cells (Fig. 9I). Finally, the most common αSMA-positive phenotypes observed were fibroblastlike cells in linear arrays similar to those presented in Figure 9I, which were completely negative for GFAP (Fig. 9J). In addition, in this case, the αSMA-positive structures were larger, fibrillar (Fig. 9K), and aligned on both sides of the nuclei (Fig. 9L).

All six specimens contained cells with the same colocalization patterns. Specifically, every specimen contained dual-positive cells reactive for GFAP and vimentin, GFAP and glutamine synthetase, and GFAP and αSMA. Similarly, every sample contained regions of GFAP-negative/αSMA-positive cells, GFAP-negative/vimentin-positive cells, and evidence of cells in transition. In response to the reviewer's concerns about the nonquantitative nature of this study, three images from each sample judged to be of high density and transitional and fibroblastic phenotypes were evaluated for tissue-associated differ-

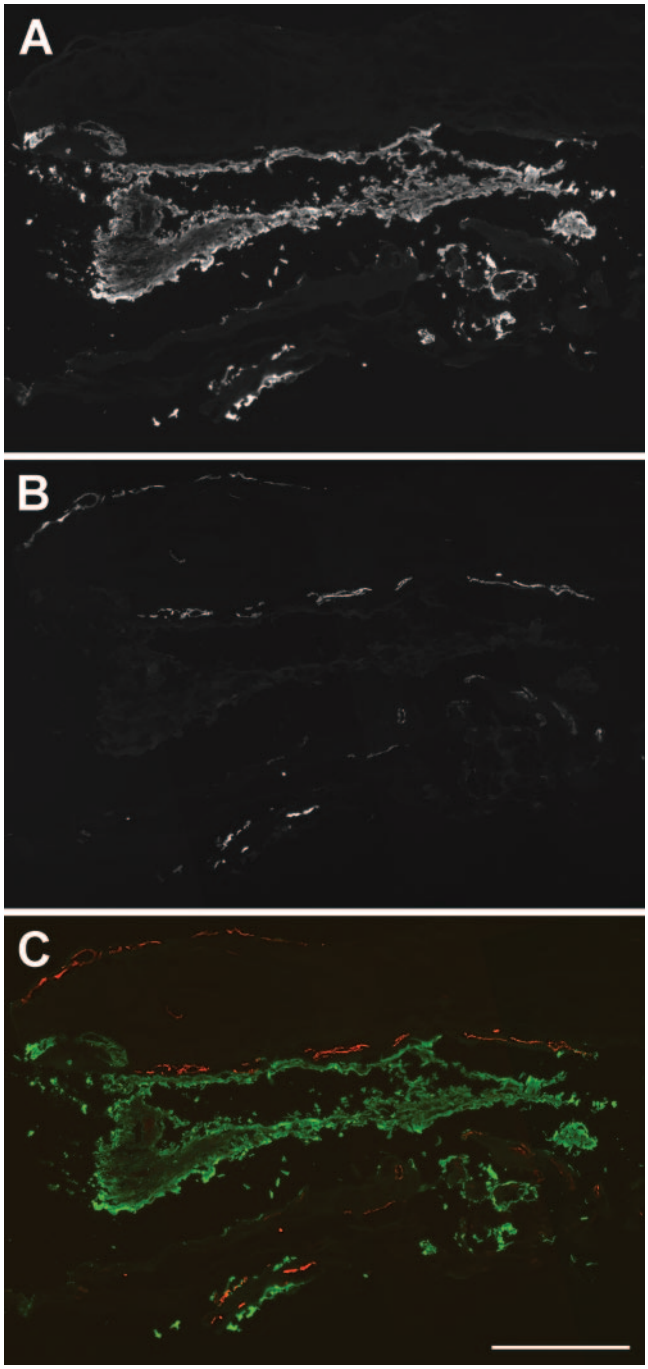

FIGURE 8. Indirect immunofluorescence evaluation of GFAP and αSMA distribution in human epiretinal scar. Cryosections adjacent to those presented in Figure 3A were double probed with antibodies against GFAP (**A**) and αSMA (**B**) and were detected with fluorochrome-conjugated secondary antibodies. (**C**) Merged image contains two color channels representing GFAP (*green*) and αSMA (*red*). Scale bar, 250 μm.

ences in pixel intensity. Results of this analysis (Table 3) are consistent with the expression changes apparent in Figures 6, 7, and 9.

DISCUSSION

Previously published studies from this laboratory demonstrated that primary cultures of freshly isolated Müller cells porcine or human retina undergo phenotype changes that include loss of the glial intermediate filament protein GFAP and de novo expression of the myoid marker αSMA.[15,16,18] These changes result in fibroblastlike cells that are immunochemically unrecognizable as of Müller cell origin. The present study extends our understanding of this phenomenon by reporting changes in glutamine synthetase content relative to the glial and myoid markers and the rapid, early changes that occur in the first week after isolation. With the use of immunochemical techniques, we improved our understanding of the three distinct stages of phenotype change that follow the isolation of Müller cells from the normal retina.[2] *Early reactive* Müller cells are positive for *normal* Müller cell marker proteins, including glutamine synthetase, GFAP, and vimentin and remain negative for αSMA. *Late reactive* Müller cells lack glutamine synthetase, are positive for GFAP and vimentin, and begin expressing αSMA. *Myofibroblastic* Müller cells are completely negative for glutamine synthetase and GFAP and are strongly positive for vimentin and αSMA. Immunochemical studies of diabetic scar identified Müller cells with the same immunochemical staining patterns and intermediate or transitional phenotypes. These observations confirmed the previously reported presence of immunochemically identifiable Müller cells in diabetic fibrocontractive disease[19,20] and the functional relevance of phenotype plasticity in culture[16,18] and confirmed that the fibroblastlike cells responsible for generating tractional forces can be derived from phenotypically altered Müller cells.

These observations are consistent with most of the previously published studies in this field. A number of investigators examined diabetic scar with the goal of identifying the causal cell types. Ultrastructural studies beginning nearly three decades ago reported the presence of glia and other cell types in diabetic epiretinal membranes.[13] The development of immunochemical techniques with antibodies against GFAP permitted positive identification of glia in these tissues by a number of different laboratories.[3,4,7,19–22] However, glia were reported to have minor roles with respect to tractional force generation,[23] a conclusion that was supported by several lines of evidence. In the study by Sramek et al.,[3] the investigators reported that GFAP reactivity in the epiretinal tissues examined correlated inversely with clinical contractility, leading the investigators to conclude that glia are unlikely to contribute to tractional force generation in these disorders. Yet another study from the same group evaluated regional variations in retinal traction compared with immunochemical characterization of the cell types in the adjacent epiretinal tissues and yielded the same general conclusion.[24] Most studies of diabetic epiretinal membranes also described the presence of fibrocytes or myofibroblasts and more recent studies confirmed these observations using antibodies against αSMA.[10–12] Based on the mechanistic association between αSMA expression and tractional force generation, there is little doubt that these cells represented the source of diabetic traction.

To our knowledge, this is the first study offering positive experimental evidence indicating that contractile, myofibroblastlike cells can be of local origin. However, it is also important to acknowledge an important limitation of this study. Although the different Müller cell phenotypes and transitional stages in diabetic scar are now documented, we are aware of no glial-specific markers that persist in the myofibroblastic phenotype. As a result of this limitation, we cannot exclude the possibility that some portion of the myofibroblastlike cells with the same immunochemical profile originated from other cells or tissues. Similarly, despite

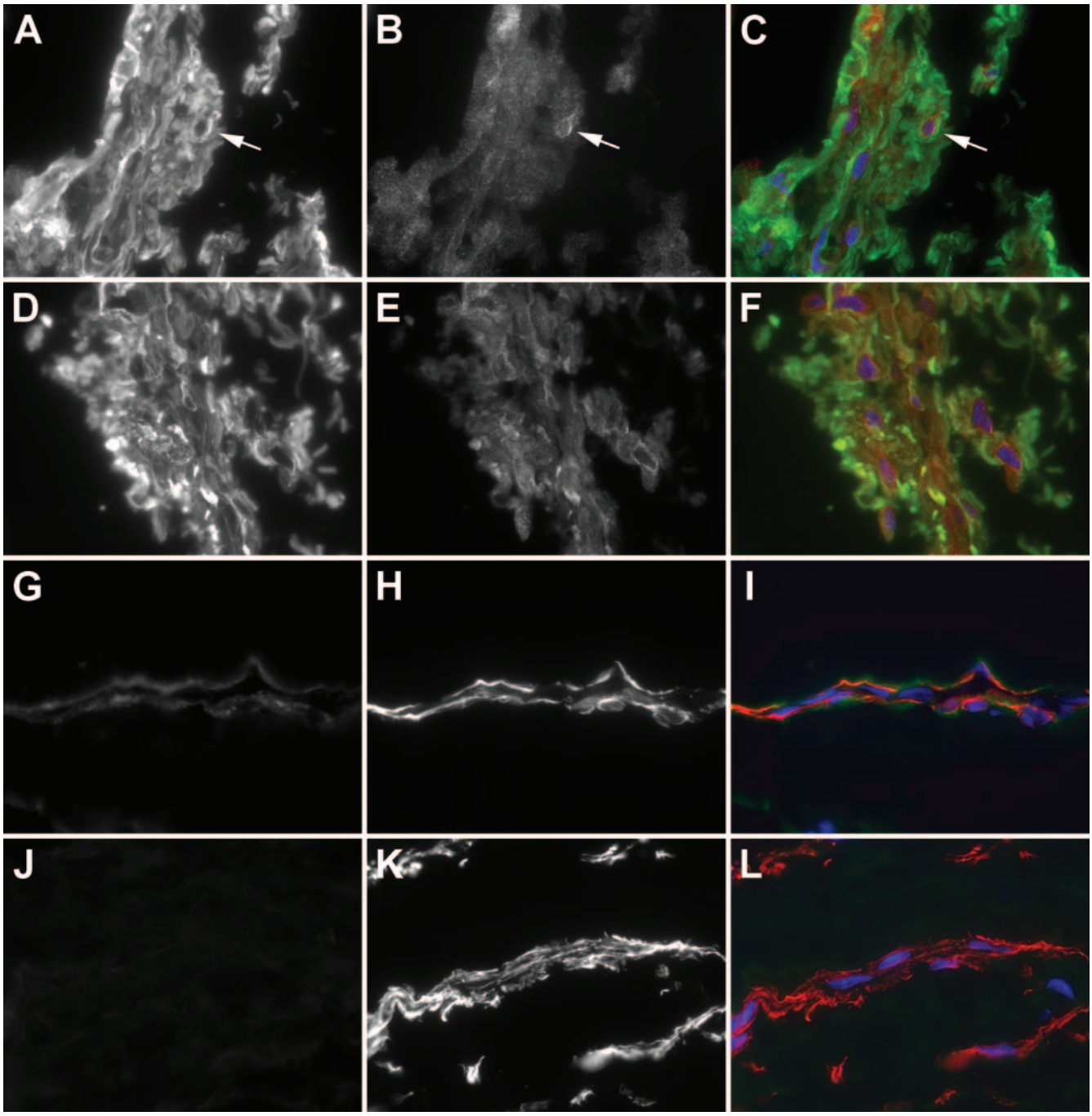

FIGURE 9. High-magnification indirect immunofluorescence evaluation of GFAP and αSMA distribution in human epiretinal scar. Cryosections were double probed as described in Figure 6 with antibodies against GFAP (**A**, **D**, **G**, **J**) and αSMA (**B**, **E**, **H**, **K**) and detected using fluorochrome-conjugated secondary antibodies. Nuclei were labeled using DAPI. (**C**, **F**, **I**, **L**) Merged images contain three color channels representing DAPI (*blue*), GFAP (*green*), and αSMA (*red*). Scale bar, 50 μm.

TABLE 3. Changes in Protein-Specific Fluorescence Intensity Associated with Phenotype

Cell Density	High Density	Transitional	Fibroblastic
GFAP	50.1 ± 17.2	37.3 ± 17.6	15.9 ± 10.4
Vimentin	50.4 ± 19.1	30.7 ± 17.5	57.9 ± 29.3
Glutamine synthetase	43.1 ± 11.9	41.7 ± 12.5	1.3 ± 0.3
αSMA	25.1 ± 9.8	46.9 ± 10.9	73.1 ± 34.0

Values are mean tissue intensities minus background ± SD.

the proximity and obvious regional changes in Müller cell phenotype, an astrocytic lineage for some of the GFAP-positive cells lacking glutamine synthetase reactivity also cannot be excluded completely.

What then is the role of Müller cells in proliferative diabetic retinopathy? These cells are known to be capable of translocating to the vitreous and have been positively identified in PDR epiretinal scar. Ample evidence indicates that Müller cells represent a functional source of several important growth factors, such as VEGF and bFGF,[25–28] and, as such, can drive the progression of fibrovascular events. It is also clear that Müller cells have the capacity to assume a myofibroblastic phenotype in disease and have the documented capacity to generate tractional force in vitro and in vivo.[15,18] Finally, the latter activity occurs in response to growth factors now known to be present in biologically active quantities in human diabetic vitreous that correlate with disease type and severity.[15,18,29] When considered together, these data constitute compelling evidence in support of myofibroblastic Müller cells as the effector population in PDR.

Finally, a PubMed search using the terms Müller and glucose yielded nine published papers examining Müller cell responses to high-glucose culture medium.[30–35] Six were studies of rMC-1, an SV40 virus-immortalized cell line established from light-damaged rat retina,[36] and reported high glucose–induced increases in apoptosis, oxidative stress, protein nitration, and protein production.[30–35] The rMC-1 is reported to be a phenotypically stable cell line[36] and is of limited relevance to our studies of early phenotype changes in primary Müller cells. Three other published studies used established cultures of primary rat and mouse Müller cells and reported high glucose–induced apoptosis mediated through Akt,[37] increases in monocyte chemotactic protein-1 secretion,[38] and, when combined with hypoxia, downregulation of VEGF production.[39] Again, these studies were of established rather than freshly isolated cells and were of limited relevance to our studies of Müller cell phenotype change. However, in most of them, cells were maintained in low-glucose medium, and glucose-induced changes were examined in response to an abrupt shift to a fivefold higher concentration. In light of the apparent absence of deleterious effects associated with continuous culture in high glucose, one cannot help but wonder to what extent the high glucose–associated responses arose from magnitude of change rather than from glucose concentration.

References

1. Frank RN. Diabetic retinopathy. *N Engl J Med.* 2004;350(1):48–58.
2. Guidry C. The role of Muller cells in fibrocontractive retinal disorders. *Prog Retin Eye Res.* 2005;24(1):75–86.
3. Sramek SJ, Wallow IH, Stevens TS, et al. Immunostaining of preretinal membranes for actin, fibronectin, and glial fibrillary acidic protein. *Ophthalmology.* 1989;96(6):835–841.
4. Hosoda Y, Okada M, Matsumura M, et al. Epiretinal membrane of proliferative diabetic retinopathy: an immunohistochemical study. *Ophthalmic Res.* 1993;25(5):289–294.
5. Mizutani M, Gerhardinger C, Lorenzi M. Muller cell changes in human diabetic retinopathy. *Diabetes.* 1998;47(3):445–449.
6. Esser P, Heimann K, Wiedemann P. Macrophages in proliferative vitreoretinopathy and proliferative diabetic retinopathy: differentiation of subpopulations. *Br J Ophthalmol.* 1993;77(11):731–733.
7. Weller M, Esser P, Heimann K, et al. Idiopathic proliferative vitreoretinopathy: activation of microglial cells as the deciding factor [in German]. *Ophthalmologe.* 1992;89(5):387–390.
8. Hiscott P, Gray R, Grierson I, et al. Cytokeratin-containing cells in proliferative diabetic retinopathy membranes. *Br J Ophthalmol.* 1994;78(3):219–222.
9. Arora PD, McCulloch CA. Dependence of collagen remodeling on alpha-smooth muscle actin expression by fibroblasts. *J Cell Physiol.* 1994;159:161–175.
10. Walshe R, Esser P, Wiedemann P, et al. Proliferative retinal diseases: myofibroblasts cause chronic vitreoretinal traction. *Br J Ophthalmol.* 1992;76(9):550–552.
11. Bochaton-Piallat ML, Kapetanios AD, Donati G, et al. TGF-beta1, TGF-beta receptor II and ED-A fibronectin expression in myofibroblast of vitreoretinopathy. *Invest Ophthalmol Vis Sci.* 2000;41(8):2336–2342.
12. Hinton DR, Spee C, He S, et al. Accumulation of NH2-terminal fragment of connective tissue growth factor in the vitreous of patients with proliferative diabetic retinopathy. *Diabetes Care.* 2004;27(3):758–764.
13. Kampik A, Kenyon KR, Michels RG, et al. Epiretinal and vitreous membranes: comparative study of 56 cases. *Arch Ophthalmol.* 1981;99(8):1445–1454.
14. Gamulescu MA, Chen Y, He S, et al. Transforming growth factor β2-induced myofibroblastic differentiation of human retinal pigment epithelial cells: regulation by extracellular matrix proteins and hepatocyte growth factor. *Exp Eye Res.* 2006;83(1):212–222.
15. Guidry C. Tractional force generation by porcine Muller cells: development and differential stimulation by growth factors. *Invest Ophthalmol Vis Sci.* 1997;38(2):456–468.
16. Guidry C. Isolation and characterization of porcine Muller cells: myofibroblastic dedifferentiation in culture. *Invest Ophthalmol Vis Sci.* 1996;37(5):740–752.
17. King JL, Guidry C. Muller cell production of insulinlike growth factor binding proteins in vitro: modulation with phenotype and growth factor stimulation. *Invest Ophthalmol Vis Sci.* 2004;45(12):4535–4542.
18. Guidry C, Bradley KM, King JL. Tractional force generation by human Muller cells: growth factor responsiveness and integrin receptor involvement. *Invest Ophthalmol Vis Sci.* 2003;44(3):1355–1363.
19. Nork TM, Wallow IH, Sramek SJ, et al. Muller's cell involvement in proliferative diabetic retinopathy. *Arch Ophthalmol.* 1987;105(10):1424–1429.
20. Guerin CJ, Wolfshagen RW, Eifrig DE, et al. Immunocytochemical identification of Muller's glia as a component of human epiretinal membranes. *Invest Ophthalmol Vis Sci.* 1990;31(8):1483–1491.
21. Ohira A, de Juan E Jr. Characterization of glial involvement in proliferative diabetic retinopathy. *Ophthalmologica.* 1990;201(4):187–195.
22. Molitor R, Esser P, Weller M, et al. Contractile elements in proliferative retinal diseases [in German]. *Ophthalmologe.* 1992;89(1):34–38.
23. Hiscott PS, Grierson I, Trombetta CJ, et al. Retinal and epiretinal glia—an immunohistochemical study. *Br J Ophthalmol.* 1984;68(10):698–707.
24. Nork TM, Wallow IH, Sramek SJ, et al. Immunocytochemical study of an eye with proliferative vitreoretinopathy and retinal tacks. *Retina.* 1990;10(1):78–85.
25. Wen R, Song Y, Cheng T, et al. Injury-induced upregulation of bFGF and CNTF mRNAS in the rat retina. *J Neurosci.* 1995;15(11):7377–7385.
26. Amin RH, Frank RN, Kennedy A, et al. Vascular endothelial growth factor is present in glial cells of the retina and optic nerve of human subjects with nonproliferative diabetic retinopathy. *Invest Ophthalmol Vis Sci.* 1997;38(1):36–47.
27. Cao W, Wen R, Li F, et al. Mechanical injury increases bFGF and CNTF mRNA expression in the mouse retina. *Exp Eye Res.* 1997;65(2):241–248.
28. Abu El-Asrar AM, Desmet S, Meersschaert A, et al. Expression of the inducible isoform of nitric oxide synthase in the retinas of human subjects with diabetes mellitus. *Am J Ophthalmol.* 2001;132(4):551–556.
29. Guidry C, Feist R, Morris R, et al. Changes in IGF activities in human diabetic vitreous. *Diabetes.* 2004;53(9):2428–2435.
30. Du Y, Sarthy VP, Kern TS. Interaction between NO and COX pathways in retinal cells exposed to elevated glucose and retina of

diabetic rats. *Am J Physiol Regul Integr Comp Physiol*. 2004; 287(4):R735–R741.

31. Kusner LL, Sarthy VP, Mohr S. Nuclear translocation of glyceraldehyde-3-phosphate dehydrogenase: a role in high glucose-induced apoptosis in retinal Muller cells. *Invest Ophthalmol Vis Sci.* 2004; 45(5):1553–1561.
32. Layton CJ, Becker S, Osborne NN. The effect of insulin and glucose levels on retinal glial cell activation and pigment epithelium-derived fibroblast growth factor-2. *Mol Vis.* 2006;12:43–54.
33. Shelton MD, Kern TS, Mi JJ, et al. Glutaredoxin regulates nuclear factor κB and intercellular adhesion molecule in Muller cells: model of diabetic retinopathy. *J Biol Chem.* 2007;282(17):12467–12474.
34. Busik JV, Mohr S, Grant MB. Hyperglycemia-induced reactive oxygen species toxicity to endothelial cells is dependent on paracrine mediators. *Diabetes.* 2008;57(7):1952–1965.
35. Zhan X, Du Y, Crabb JS, et al. Targets of tyrosine nitration in diabetic rat retina. *Mol Cell Proteomics.* 2008;7(5):864–874.
36. Sarthy VP, Brodjian SJ, Dutt K, et al. Establishment and characterization of a retinal Muller cell line. *Invest Ophthalmol Vis Sci.* 1998;39(1):212–216.
37. Xi X, Gao L, Hatala DA, et al. Chronically elevated glucose-induced apoptosis is mediated by inactivation of Akt in cultured Muller cells. *Biochem Biophys Res Commun.* 2005;326(3):548–553.
38. Harada C, Okumura A, Namekata K, et al. Role of monocyte chemotactic protein-1 and nuclear factor kappa B in the pathogenesis of proliferative diabetic retinopathy. *Diabetes Res Clin Pract.* 2006;74(3):249–256.
39. Brooks SE, Gu X, Kaufmann PM, et al. Modulation of VEGF production by pH and glucose in retinal Muller cells. *Curr Eye Res.* 1998;17(9):875–882.